Engineering Journal issn: 0125-8281

Article

Finite Element Analysis on Reinforced Concrete Columns Strengthened by ECC Jacketing under Eccentric Compressive Load

Mohammad Javad Memar[1,a], Ali Kheyroddin[2,b,*], and Ali Hemmati[3,c]

1 Department of Civil Engineering, Semnan Branch, Islamic Azad University, Semnan, Iran
2 Department of Civil Engineering, Semnan University, Semnan, Iran
3 Seismic Geotechnical and High Performance Concrete Research, Department of Civil Engineering, Semnan Branch, Islamic Azad University, Semnan, Iran
E-mail: [a]mohammadjavadmemar@gmail.com, [b]kheyroddin@semnan.ac.ir (Corresponding author), [c]ali.hemmati@semnaniau.ac.ir

Abstract. Engineered cementitious composite (ECC) can be used for strengthening of concrete columns due to its similar structure and suitable connection to normal concrete and its special tension behavior. In this study, to analyse the columns, finite element (FE) method was used after verification by experimental results. Reference column was strengthened by normal concrete and ECC jacketing. The effects of type of jacket material, longitudinal reinforcement, compressive stress and ultimate tensile strain of ECC on variations of eccentric load-bending moment (P-M) interaction curves were investigated. Results showed that the use of ECC instead of normal concrete can increase load carrying capacity of strengthened column, due to tensile strain hardening behavior of this material. It was found that, amount of this increase depends on eccentricity of eccentric load and varying from 0.4-23%. In ECC jacketing, tensile cracks are continuous, but in concrete jacketing, there were discrete cracks and more quantity of damages. Due to higher load carrying capacity and better distribution of tensile cracks in ECC jacketing than normal concrete jacketing, the use of ECC is suitable for strengthening of reinforced concrete columns. Load carrying capacity of columns under concentric load and pure bending moment were calculated by theoretical method and the results were compared with FE.

Keywords: Strengthened column, ECC jacketing, eccentric load, P-M interaction curves, finite element.

ENGINEERING JOURNAL Volume 24 Issue 5
Received 13 September 2019
Accepted 15 February 2020
Published 30 September 2020
Online at https://engj.org/
DOI:10.4186/ej.2020.24.5.77

DOI:10.4186/ej.2020.24.5.77

1. Introduction

Concrete columns, as main members in moment frame system should not be failed and damaged before the beams (weak beam-strong column theory) [1], so it is necessary to strengthened reinforced concrete columns that to not meet new seismic provisions. There are a variety of methods for strengthened of concrete columns including the use of jacketing: reinforced concrete [2, 3], fiber reinforced polymer (FRP) [4, 5], steel [6, 7], and combination of these methods [8]. Each method has its advantages and disadvantages. FRP jacketing increases compressive strength and ductility in concrete column but at eccentric load with high eccentricity or high lateral load, FRP layers fail earlier [9]. The use of steel jacketing can lead to confinement for concrete core and increased column ductility [10]. But, it is weak against corrosion and fire. Concrete jacketing because of its similarity to reference column material and its suitable connection may be appropriate, but weakness of concrete in tension and its hard application are disadvantages of this method. If concrete-like materials were used and tensile behavior of concrete improves, then this method of strengthened of concrete columns can also be improved.

In the recent years, materials including engineered cementitious composite (ECC) or high performance fiber reinforced cementitious composite (HPFRCC) have been introduced lacking coarse grain. ECC behavior is almost similar to that of concrete under pressure but is quite different from that under tension. This different behavior of ECC or HPFRCC under tension compared to concrete is due to presence of PVA (ploy vinyl alcohol) fibers in structure of this material. Presence of fibers in this material with bridging between cracks leads to strain hardening under tension [11, 12]. As can be seen in Fig. 1, ECC has a different behavior to normal concrete and fiber reinforced concrete (FRC) under tension.

ECC is considered as a high-performance material because of strain hardening behavior after initial cracking. ECC and concrete have almost similar ranges of tensile stress (3-6 MPa) and compressive stress (20-90 MPa), but they are different in terms of tensile strain. Ultimate strain in ECC is equal to 2-8%, attributing to failure of concrete in a brittle behavior of primary cracking, but in ECC, after primary cracking, stress increases until reaching ultimate strain and then it has a softening behavior [13].

Numerous studies have been done on members made of ECC or HPFRCC. Yuan et al. compared columns made of concrete and ECC under eccentric load in terms of load carrying capacity by experimental and theoretical methods. They showed a difference between load carrying capacity of the two columns at low eccentricity close to each other and it increased at high eccentricity [14]. Quang et al. applied axial load and horizontal biaxial load on concrete columns and HPFRCC, and evaluated both flexure and shear failure modes for column.

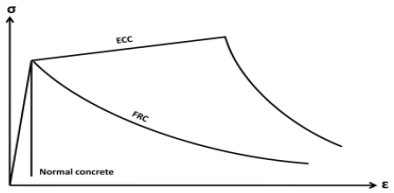

Fig. 1. Comparison of tension stress-strain curve of normal concrete, fiber reinforced concrete (FRC) and ECC [12].

They showed an increase in lateral load capacity by 40 and 10% ductility in the column made of HPFRCC compared to the concrete column [15]. Jinlong et al. using finite element (FE) and theoretical methods studied ECC column under eccentric load. Maximum error between these methods for ECC column was equal to 8.2% [16]. Hemmati et al. Using experimental methods and finite element by ABAQUS software studied the effect of HPFRCC on frame by considering three frames of normal concrete, HPFRCC, and the frame consisting of normal concrete and HPFRCC. Difference between amount of lateral load in experimental methods and finite element results was obtained as 4.5 and 2.8%, respectively for concrete and HPFRCC frames [17]. Use of ECC due to, strength capacity under tension, ductility [15, 17], and durability (due to lack of coarse grain) [18, 19] increased than normal concrete, as ECC was applied instead of concrete for strengthened of concrete members. Also due to similarity of ECC structure to concrete, a strong connection can be made between ECC jacketing and primary concrete body. Shim et al., Meda et al used HPFRCC (ECC) jacketing for strengthened of reinforced concrete column under lateral load. They showed that, this technique is suitable for repairing and strengthening of reinforced concrete columns [20, 21].

In this study, reinforced concrete column is strengthened by concrete and ECC jacketing. The effects of variables including type of jacket material, longitudinal reinforcement, compressive stress of ECC, and ultimate tensile strain of ECC, on eccentric load–bending moment (P-M) interaction curve is investigated in strengthened columns. To more exactly evaluate P-M interaction curve in region of pressure, region of tension and balance point, each column is subjected to concentric load, pure bending moment and different eccentric loads.

2. Review of Experimental Study and FE Analysis

Due to high number of columns and low distance of eccentricity in eccentric loads (about 20 mm), the finite element method was used to analyse the columns. To verify modelling of concrete, ECC, and steel reinforcement in software, first finite element results need to be compared and verified by experimental results. Finally, finite element results are compared with theoretical results for circular columns under concentric load and pure bending moment.

2.1. Detail of Experimental Columns and Loading System

Yuan et al. made reinforced concrete (called as C) and reinforced ECC (called as E) columns. Column length was equal to 1200 mm (consisting of two haunch connections for applying eccentric load and main column length) and effective cross section was equal to 200*250 mm as shown in Fig. 2. Columns under eccentric compression load had an eccentricity of 120 mm. Test results showed that peak of compressive stress of concrete and ECC was equal to 32.28 and 46.08 MPa, respectively. Longitudinal reinforcement was 4Φ16 and transverse reinforcement was Φ8@100 mm. Table 1 presents mechanical properties for steel reinforcement. Figure 3 shows stress-strain curve of ECC under tension [14].

In Table 1, D is diameter of steel reinforcement, f_y is yield stress of steel reinforcement, f_u is ultimate of steel reinforcement and E_s is elastic module of steel reinforcement.

2.2. Material Modelling and Stress-Strain Curves

In general, the ABAQUS software [22] can be used to define nonlinear behavior of concrete and cement composites from three behavioral models in the software. These methods include: 1- concrete smeared cracking, 2- brittle cracking, and 3- have used this software to simulate concrete and ECC applied concrete damaged plasticity [23]. In this model, it is possible to enter different points of stress-strain curve of normal concrete and ECC under compression and tension [24, 25]. Here in, two concrete failure mechanisms were predicted: the first one is tension cracking and the second one is compression cracking. Compression behavior of concrete and ECC is almost similar to each other but it has different under tensions. Figure 4 shows stress-strain curve (compression and tension) for concrete, ECC, and steel. Solid element was used for modelling of concrete and ECC. Truss elements were used to model steel reinforcements [26 - 28].

Equation (1) shows stress-strain relationship for concrete under compression. Eq. (2) and Eq. (3) are related to stress-strain relationship for ECC under compression and tension, respectively. Equation (4) is related to steel under compression and tension [14, 16].

For concrete: (under compression)

$$\sigma_c = f_c^{'}\left[2.(\frac{\varepsilon}{\varepsilon_c^{'}}) - (\frac{\varepsilon}{\varepsilon_c^{'}})^2\right] \xleftarrow{if} 0 \le \varepsilon < \varepsilon_c^{'} \qquad (1)$$

$$\sigma_c = f_c^{'}\left[1 - \frac{\varepsilon - \varepsilon_c^{'}}{\varepsilon_{cu}^{'} - \varepsilon_c^{'}}\right] \xleftarrow{if} \varepsilon_c^{'} \le \varepsilon < \varepsilon_{cu}^{'}$$

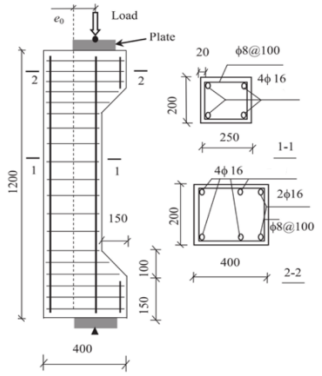

Fig. 2. Detail of experimental columns(C&E) [14].

Table 1. Mechanical property of steel reinforcement in C and E columns [14].

D (mm)	f_y (MPa)	f_u (MPa)	E_s (GPa)
8	359	525	195
16	527	621	201

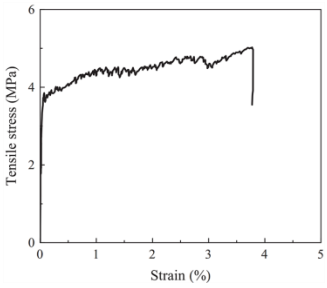

Fig. 3. Tension stress-strain curves of ECC [14].

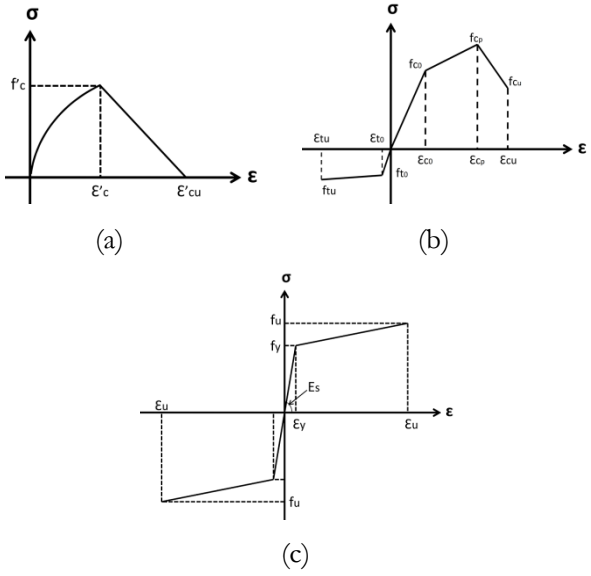

Fig. 4. Stress-strain curves for: (a) concrete under compression; (b) ECC under compression and tension; (c) steel under compression and tension.

For ECC: (under compression)

$$\sigma_{Ec} = \frac{\varepsilon}{\varepsilon_{c0}} . f_{c0} \xleftrightarrow{if} 0 \le \varepsilon < \varepsilon_{c0} \quad (2)$$

$$\sigma_{Ec} = f_{c0} + (\frac{f_{cp} - f_{c0}}{\varepsilon_{cp} - \varepsilon_{cu}})(\varepsilon - \varepsilon_{c0}) \xleftrightarrow{if} \varepsilon_{c0} \le \varepsilon < \varepsilon_{cp}$$

$$\sigma_{Ec} = f_{cp} + (\frac{f_{cu} - f_{cp}}{\varepsilon_{cu} - \varepsilon_{cp}})(\varepsilon - \varepsilon_{cp}) \xleftrightarrow{if} \varepsilon_{cp} \le \varepsilon < \varepsilon_{cu}$$

For ECC: (under tension)

$$\sigma_{Et} = \frac{\varepsilon}{\varepsilon_{t0}} f_{t0} \xleftrightarrow{if} 0 \le \varepsilon < \varepsilon_{t0} \quad (3)$$

$$\sigma_{Et} = f_{t0} + (\frac{f_{tu} - f_{t0}}{\varepsilon_{tu} - \varepsilon_{t0}})(\varepsilon - \varepsilon_{t0}) \xleftrightarrow{if} \varepsilon_{t0} \le \varepsilon < \varepsilon_{tu}$$

For steel: (under compression and tension)

$$\sigma_s = E_s \varepsilon \xleftrightarrow{if} 0 \le \varepsilon < \varepsilon_y \quad (4)$$

$$\sigma_s = f_y + (f_u - f_y).(\frac{\varepsilon - \varepsilon_y}{\varepsilon_u - \varepsilon_y}) \xleftrightarrow{if} \varepsilon_y \le \varepsilon < \varepsilon_u$$

In Eq. (1) to Eq. (4), σ_{cc} is compressive stress of concrete, ε is strain of material, f_c' is peak compressive stress of unconfined concrete, ε_c' is compressive strain of unconfined concrete at peak stress, ε_{cu}' is ultimate compressive strain of unconfined concrete, σ_{cE} is compressive stress of ECC, f_{c0} is maximum elastic compressive stress of ECC, ε_{c0} is maximum elastic compressive stain of ECC, f_{cp} is peak compressive stress of ECC, ε_{cp} is compressive strain of ECC at peak stress, f_{cu} is ultimate compressive stress of ECC, ε_{cu} is ultimate compressive strain of ECC, σ_{Et} is tensile stress of ECC, f_{t0} is initial cracking tensile stress of ECC, ε_{t0} is initial cracking tensile strain of ECC, f_{tu} is ultimate tensile stress of ECC, ε_{tu} is ultimate tensile strain of ECC, σ_s is stress of steel reinforcement, ε_y is yield strain of steel reinforcement, $\varepsilon_u$is ultimate strain of steel reinforcement. In linear elastic regime, the Young's modulus of concrete (E_c) and ECC (E_E) was calculated using Eq. (5) and Eq. (6), respectively [16, 29, 30].

$$E_c = 4730\sqrt{f_c'} \quad (5)$$

$$E_E = \frac{f_{c0}}{\varepsilon_{c0}} \quad (6)$$

2.3. Simulations C and E Columns for FE Analysis

Column simulation in software was performed according to experimental conditions. To apply boundary conditions on the column, top and bottom columns were selected and rotation and axial displacement (in accordance with experimental conditions) were free. For loading, axial displacement of 10 mm/sec was applied to reference points of the column with a certain eccentricity. To perform FE analysis, the column should be meshed. It is noteworthy that, dimension of the mesh can influence results of column analysis, highlighting dependency to the mesh dimension [25]. If the mesh size is very large, the concrete or ECC will face with late tensile cracking and resistance and ductility of the column will be more than reality, and if the mesh size is too small, concrete will soon face with tensile cracking and resistance and ductility of the column will be less than reality [31]. Figure 5(a) shows boundary conditions and position reinforcement for C and E columns. In this study, due to applying finite element analysis for similar column [27], meshing sizes is equal to 50 mm for analysis of columns as shown in Fig. 5(b).

As steel reinforcements often have a small diameter and area, distribution of stress is usually uniform. As a result, their behavior can be modelled by one-dimensional elements with a one-axial stress theory (truss). It is clear that, degrees of freedom of rebar should not be independent of degrees of freedom for its surrounding concrete or ECC. To accommodate this, a property called embedded is included in the software [26]. Using this property, a piece can be placed in the other part so that, degrees of freedom of inner parts are determined using its surrounding degrees of freedom.

2.4. Verifications FE Results for C and E Columns with Experimental Results

Columns C and E were analysed using finite element method and were compared with experimental results for verification of results. Figure 6 shows axial load–axial strain curve of columns. Axial strain measures the point under eccentric load. Figure 7 shows eccentric load-lateral deflection curves. Lateral deflection measures mid-height (f) of the column. As shown in Fig. 7, in elementary parts of eccentric load-lateral deflection curve, simulated sample results are harder than experimental results, the reason of to lower degrees of freedom in simulation models than experimental samples [32]. Figures 8 and 9 show compressive and tensile damages of the two columns C and E, respectively, as well as comparison of results obtained from experimental and FE methods. Degradation of elastic stiffness in columns was determined by two damage variables, namely damage compact (dc) and damage tensile (dt), which are functions of plastic strain, temperature, and field variables [28]. These damages in column C were also greater than in column E in terms of surface of cracks and quantities of damages. There was close difference between compressive damages of the two columns, due to similarity of behavior between concrete and ECC under pressure. Due to different behavior of two materials under tension, tensile damages for C column were discrete and for E column,

were continuous. Acceptable conformity was found between compressive and tensile damages of two columns as obtained by experimental and FE methods.

In general, as illustrated in Fig. 7, numerical simulation method is not capable of simulating load loss and downward branching of load-displacement curve under present conditions and the solution diverges immediately after crushing of concrete or ECC under compact. To simulate drop load and descending branch of curve, it is necessary to use the theories of fracture mechanics and to apply higher viscosity values. However, as shown in Fig. 7, upward branch of load-displacement curve has been well simulated and peak load and its corresponding displacement has been correctly determined. Error for peak load was equal to 0.8 and 5.2%, respectively as obtained for FE method compared to experimental method for concrete and ECC columns, indicating accuracy of FE method.

In addition, the experimental and numerical axial load-displacement curves shown in Fig. 6 and Fig. 7 are also in good agreement. On this basis, it can be concluded that the methods and theories used are able to simulate the behavior of the columns until the process of corrosion of the concrete and ECC, failure of columns, and load carrying capacity of columns.

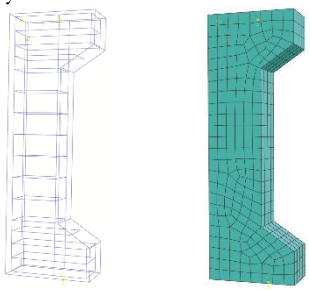

(a) (b)

Fig. 5. Simulation C and E columns: (a) boundary conditions and reinforcement position; (b) mesh size.

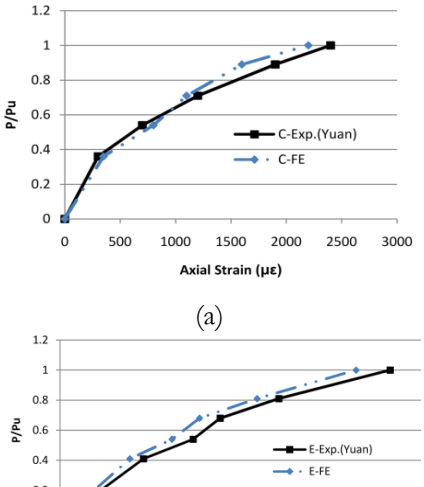

(a)

(b)

Fig. 6. Eccentric load–axial strain curves: (a) C column; (b) E column.

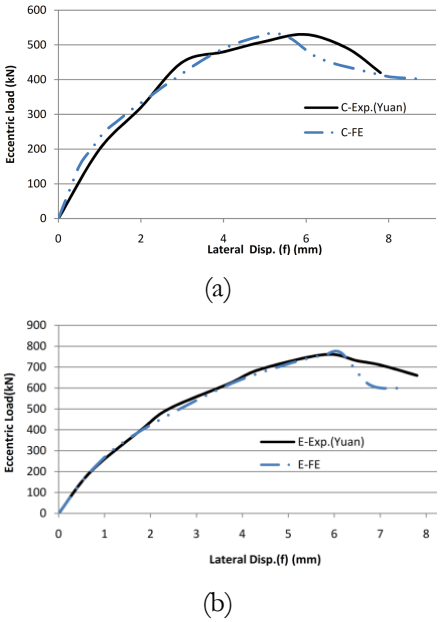

(a)

(b)

Fig. 7. Eccentric load–lateral deflection curves: (a) C column; (b) E column.

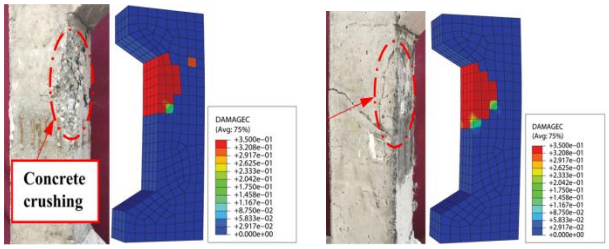

(a) (b)

Fig. 8. Crack pattern and damage quantification at compact for: (a) C column; (b) E column.

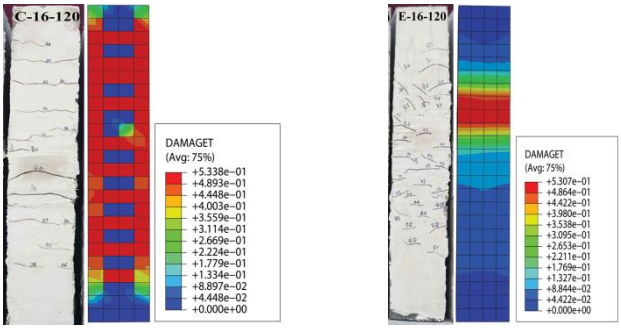

(a) (b)

Fig. 9. Crack pattern and damage quantification at tensile for: (a) C column; (b) E column.

3. Analytical Models

Purpose of this study is investigating eccentric load-bending moment (P-M) interaction curve, so the columns were considered short. Therefore, the reference reinforced concrete column (R) was 1000 mm long with 250 mm diameter, in which the effect of buckling in the column was ignored. According to ACI 318 [29], the reference column slenderness ratio $(\frac{kl_u}{r})$ is equal to 16. Because, this

value is below 22, the reference column is considered a short column.

Compressive stress concrete of R column was equal to 25 MPa. Figure 10(a) shows amount and position of longitudinal and transverse reinforcement in the reference column. The R column was strengthened and named using normal concrete or ECC jacketing as shown in Fig. 10(b) and Table 2. The ϱ value, which is ratio of total area of longitudinal reinforcement to area of the column, longitudinal reinforcement in the reference column is designed so that, ϱ value (1.4%) should not be less than recommended value of ACI (1%) [29]. In strengthened columns, amount of longitudinal reinforcement is designed such that, ϱ value should be equal to the reference column. But for columns, in which the effect of longitudinal reinforcement is studied on behavior of strengthened column, ϱ value must be changed. Cover on longitudinal reinforcement for reference column and strengthened columns are equal to 25, 30 mm, respectively.

To make a better comparison between normal concrete and ECC, thickness of the jacket in strengthened columns was constant and equal to 50 mm. Value of yielding and ultimate stress for longitudinal reinforcement was equal to 320 and 500 MPa, respectively, and transverse reinforcement was equal to 220 and 380 MPa, respectively. Elastic modulus of steel reinforcement was equal to 200 GPa. Transverse reinforcement in jacketing of strengthened column was equal to Φ8@150 mm. Based on results obtained from experimental studies on ECC or HPFRCC [14, 16, 33], mechanical properties of ECC regarding simulation in the software under compression and tension were provided in Table 3.

Each column was subjected to loads: 1- concentric load, 2- eccentric load with eccentricity of 40, 80, 100, 120, 140, 175, and 220 mm, and 3- pure bending moment. All the points mentioned in previous section for modelling of columns C and E are true here.

It is noteworthy that, interaction effect is between body of the main column with jacket around the column in reality and its correct simulation in the software.

Connection of a core column with a concrete jacket in reality was achieved by clearing and sandblasting of periphery of the core column. As a result, connection between the core column and the concrete or ECC jacket was made perfectly [2].

To simulate this behavior in the software, proper interaction between these two surfaces should be done so as to model it without the need for separation and real behavior. As shown in Fig. 11, interaction between these two surfaces (body of the reference column and concrete or ECC jacketing) was made through module interaction and by creating new constraint in model and tying them together [26].

Boundary conditions and reinforcement position for reference and strengthened circular columns were shown in Fig. 12. Meshing size was equal to 50 mm for analysis of columns. To apply boundary conditions to the column, a reference point was defined at top and bottom of the column. The column boundary conditions must be changed to apply load to the column. To apply concentric load, pure bending moment the reference point of axial displacement, rotation of 10 mm/sec, 5 rad/sec, respectively should be entered. For eccentric load, the reference point must be changed into amount of eccentricity of load.

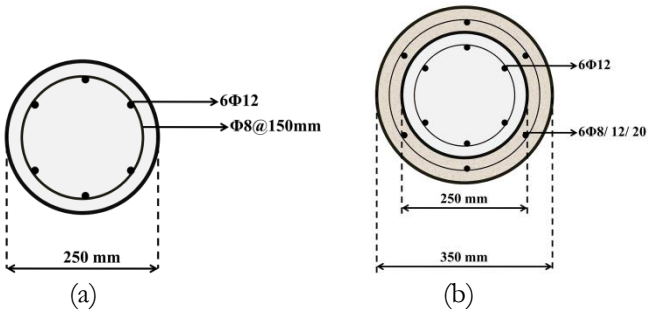

Fig. 10. Detail of circular columns: (a) reference (R) column; (b) strengthened columns with reinforced concrete or ECC jacketing.

Table 2. Strengthened columns with normal concrete or ECC jacketing. (*: longitudinal reinforcement in jacketing of strengthened column).

Column	material jacketing	f'_c (MPa)	f_{cp} (MPa)	L.R.*	ϱ%
RJRC	Concrete	35	-	6Φ12	1.4
RJRE1	ECC1	-	35	6Φ8	1
RJRE2	ECC1	-	35	6Φ12	1.4
RJRE3	ECC1	-	35	6Φ20	2.7
RJRE4	ECC2	-	25	6Φ12	1.4
RJRE5	ECC3	-	35	6Φ12	1.4

Table 3. Mechanical property of ECC at compression and tension (all unites for stress is MPa).

ECC	ECC1	ECC2	ECC3
f_{c0}	23.5	18.5	23.5
ε_{c0}%	0.1	0.08	0.1
f_{cp}	35	25	35
ε_{cp}%	0.22	0.2	0.22
f_{cu}	14	12	14
ε_{cu}%	0.32	0.3	0.32
f_{t0}	3.7	3.1	3.7
ε_{t0}%	0.021	0.015	0.021
f_{tu}	5	4.5	5
ε_{tu}%	4.5	4.5	3

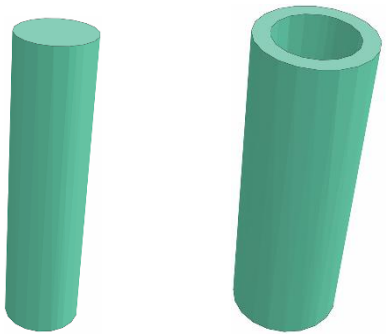

(a) (b)

Fig. 11. Modelling element columns in software: (a) core column; (b) concrete or ECC jacketing.

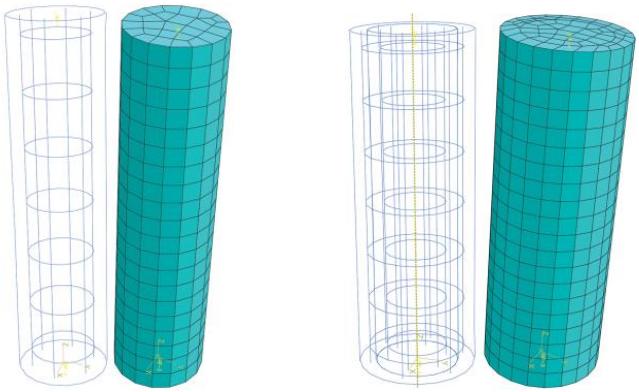

(a) (b)

Fig. 12. Simulation of circular columns; boundary conditions, reinforcement position and mesh size for: (a) reference column; (b) strengthened columns.

The confinement effect on strengthened columns with concrete or ECC jacketing is due to lateral pressures caused by transverse reinforcement of column [34]. In strengthened column with ECC jacketing, in addition to transverse reinforcement, the fibers in ECC jacketing are also effective in enhancement of confinement effect [12]. Confinement effect leads to increased compressive stress and compressive strain of concrete in confined area. There are several equations for modelling increase in compressive stress of confined concrete by transverse reinforcement [34]. In this study, FIB model code [35] was used according to Eq. (7) and Eq. (8). The diameter of confined area by transverse reinforcement in circular column is obtained from this relation ($d_i - \frac{s}{2}$) [36].

Campione considered the effect of fibers on enhancement of confinement in fiber reinforced concrete with a fictitious reduction of space between transverse reinforcement. It has been stated that, amount of this fictitious reduction depends on length (l_f), diameter (D_f) and volume percentages (v_f) of fibers [36]. In this study, due to geometrical properties ($\frac{l_f}{D_f} = 120$) and volume percentages ($v_f = 2\%$) of PVA fibers in ECC jacketing, the space between external transverse reinforcement fictitiously reduced by 16%.

In Eq. (7) and Eq. (8), f_{le} is lateral pressure of stirrups and for circular columns with conventional stirrups, it is calculated from Eq. (9), the value of k_1 is equal to 4.1 [36].

$$f_{cc}^{'} = f_c^{'}\left[1+3.5(\frac{f_{le}}{f_c^{'}})^{0.75}\right] \quad (7)$$

$$\varepsilon_{cc}^{'} = \varepsilon_c^{'}\left[1+5k_1(\frac{f_{le}}{f_c^{'}})^{0.7}\right] \quad (8)$$

$$f_{le} = \frac{2A_{s,t}\cdot f_{y,t}}{s_l d_i}\left[1-\frac{s_l}{d_i}\right]^2 \quad (9)$$

In Eq. (7) to (9), $f_{cc}^{'}$ is peak compressive stress of confined concrete, $\varepsilon_{cc}^{'}$ is compressive strain of confined concrete at peak stress, $A_{s.t}$ is area of transverse reinforcement, $f_{y.t}$ is yielding stress of transverse reinforcement, d_i is diameter of circular stirrups, s is clear spacing between stirrups, s_l is clear spacing between stirrups after fictitious reduction. To apply confinement effect in finite element analysis, stress-strain curve of concrete in confined area (diameter of confined area for strengthened columns is almost 250 mm) must be modified according to Eq. (7) and Eq. (8). As can be seen in Eq. (9), amount of lateral pressure depends on space and diameter of stirrups. If space of stirrups is large and diameter of stirrups is small, then this pressure is minimized in confined concrete area.

4. Results and Discussion

4.1. Concentric and Eccentric Load

Each column was analysed by finite element method. In this section, results are presented, and columns were compared with each other. Figures 13 and 14 shows concentric load-axial displacement curve and eccentric load-eccentricity curve of each column, respectively. After crushed of columns under pressure, downward branch of the load-displacement curve dropped, this behavior was also observed in column analysis by finite element method in study of Elchalakani et al. [27]. Reason of this solution was diverged. But the purpose of this study is to determine peak load of columns before was crushed one can be sure of the results. Due to similar behavior of concrete and ECC under compression, and geometrical and mechanical properties of the two columns of RJRC and RJRE2, concentric load-axial displacement curve of these two columns was matched as illustrated in Fig. 13. Tables 4 and 5 present exact amount of axial load and bending moment for each column, respectively. As shown in Table 6, load carrying capacity of each strengthened column was compared with the reference column. Means e=∞ presented in Tables 5 and 6 denotes pure bending moment (P_e=0) on columns. Amount of load carrying capacity in strengthened columns increased compared to the

reference column. Amount of this increase is variable and depends on type of strengthened and eccentricity of eccentric load. Because, in each level of strengthened of column, a longitudinal reinforcement was applied in the column jacketing and in four levels of strengthened of columns, ECC was used as internal material of the jacket that increases bending capacity is more than axial compressive load capacity. Such that, by increasing eccentricity of eccentric load in a particular strengthened of column, load carrying capacity difference becomes larger than the reference column. The effect of longitudinal reinforcement and ECC material on the jacket in increasing load carrying capacity of the reference column in bending mode is more than compressive mode. In all columns with increasing eccentricity, the value of eccentric load decreases. The reason is creation of a bending moment in addition to the axial load in large of eccentricity.

The difference between columns of RJRC and RJRE2 in Fig. 14(a) is visible at large eccentricity. When eccentricity of axial load increases, tension occurs at the cross-section of the columns. As a result, the difference between concrete and ECC is evident at this time. The tensile behavior of ECC varies respect to the concrete. In ECC unlike concrete after the first tensile crack was formed, the tensile strain hardens. That causes it load carrying capacity in RJRE2 column between 0.4 and 23% higher than is RJRC column. The increase in the amount of longitudinal reinforcement in the column jacketing, is effective both at large and small eccentricity (Fig. 14(b)). The effects of compressive stress and ultimate tensile strain on ECC are important at small and large eccentricity, respectively (Fig. 14(c) and Fig. 14(d)).

4.2. P-M Interaction Curves

Figure 15 shows eccentric load-bending moment (P-M) interaction curves for the reference column and strengthened columns and their comparison with each other.

P-M interaction curve is composed of three main points: concentric load (P_0), eccentric load in eccentricity of balance (P_b), pure bending moment (M_0), and two regions of pressure control and tension control. In a balance state, pressure and tensile failure to occur together in the column. Ultimate compressive strain of concrete or ECC under pressure reachesε'_{cu} or ε_{cu} respectively, at the same time, tensile strain of tensile steel reinforcement and ECC under tension is ε_y and ε_{tu}, respectively. At eccentricity less than balance eccentricity (pressure control region), failure occurs under pressure and the column has more compressive behavior. But, at eccentricity more than balance eccentricity (tension control region), failure occurs under tensile and the column has more bending behavior.

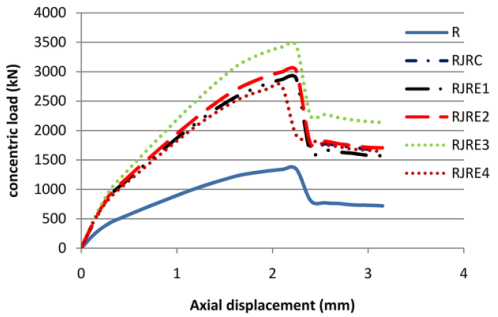

Fig. 13. Concentric load-axial displacement curves.

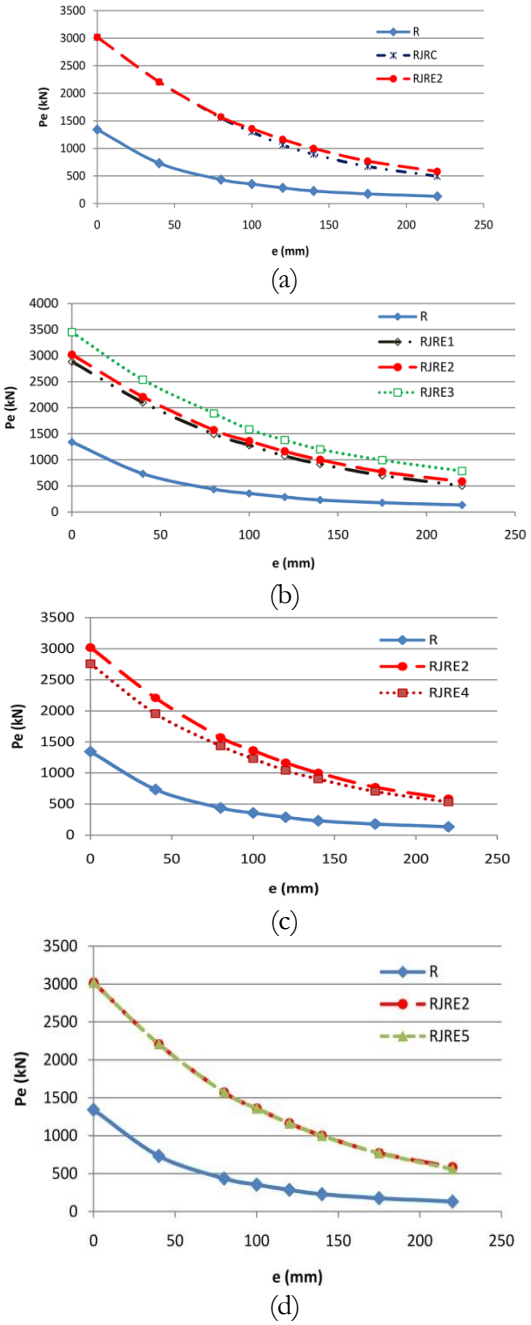

Fig. 14. Eccentric load-eccentricity curves: (a) the effect type of jacketing material; (b) the effect of longitudinal reinforcement; (c) the effect of compressive stress; (d) the effect of ultimate tensile strain.

If the member undergoes a pure bending moment before yielding tension for steel reinforcement, and an axial load is added to it, compressive stresses induced by this load will reduce tension stresses and sum of the two stresses will be lower than yielding steel reinforcement rate. As a result, an additional bending moment can now be added to the cross section to an extent that steel reinforcement stress resulted from axial load and bending moment increases and reaches amount of yielding, explaining the fact that, why increasing eccentric load increases section's moment capacity in tension control region, while in pressure control region, the opposite is true. Given that appearance of axial compression load in tension control region adds to bending capacity of the section, in calculating bending capacity of the cross section, amount of axial load, which is 100% available should be considered.

Figure 15(a) shows difference between concrete and ECC in the jacket material used for strengthened of reinforced concrete column. To make a more correct comparison between these two jacket materials, variables including jacket thickness, compressive stress, number and diameter of steel reinforcement are constant in two columns of RJRC and RJRE2. In pressure region of P-M interaction curves, load carrying capacity of these columns is almost similar. In balance point and tension region of P-M interaction curves, as ECC showed hardening in tensile behavior after the first tension crack the concrete was not resistant under tension (change in tensile behavior of concrete than ECC), that led to bridging of tensile cracks of ECC by existing fibers, and increased load carrying capacity of RJRE2 column than RJRC column. Due to higher tensile strength of column RJRE2 than RJRC, balance eccentricity becomes higher in P-M curves. Balance eccentricity of columns of RJRC and RJRE2 is equal to 100 and 140 mm, respectively.

Figure 15(b) shows the effect of longitudinal reinforcement on P-M interaction curves. Effect increased longitudinal reinforcement at the jacket layer in both pressure and tensile regions of P-M interaction curve are evident. However, the effect of this increase is greater in tensile region of P-M curve than pressure region. For example, in RJRE1 and RJRE3 strengthened columns, the area of longitudinal reinforcement was found to increase by 6.25 times. Concentric load and pure bending moment increased by 19 and 92%, respectively. This is due to greater effect of longitudinal reinforcement on flexural strength of the column than its compressive strength. For this reason, by increasing longitudinal reinforcement, balance eccentricity becomes larger in P-M interaction curves.

For columns of RJRE1, RJRE2, and RJRE3, eccentricity of balance is equal to 120, 140, and175 mm, respectively.

Figure 15(c) shows the effect of compressive stress (f_{cp}) in ECC on P-M interaction curves. By decreasing compressive strength of ECC to 10 MPa, concentric load and bending moment in column RJRE4 reduced by 9.1 and 5.6%, respectively compared to column RJRE2. Of course, there is a need for careful consideration of these two columns, as the decrease in the compressive strength of the jacket ECC caused a decrease in initial cracking of ECC under tensile stress (f_{to}) by 19%. For this reason, difference between P-M interaction curves of these two columns is evident both in pressure and tension control regions.

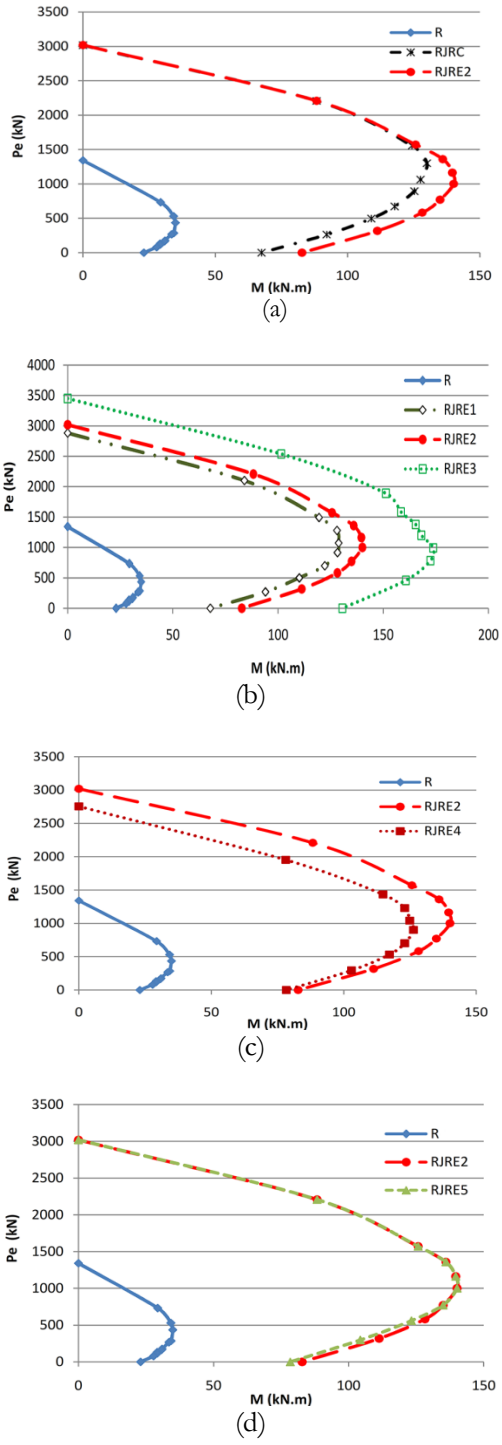

Fig. 15. Eccentric load-bending moment (P-M) interaction curves: (a) the effect type of jacket material; (b) the effect of longitudinal reinforcement; (c) the effect of compressive stress; (d) the effect of ultimate tensile strain.

For investigating the effect of ultimate tensile strain value ε_{tu} decreased from 4.5% in column RJRE2 to 3% in column RJRE5. Decreased ultimate tensile strain was ineffective in pressure control region of P-M interaction curves as shown in Fig. 15(d). But, in tension control region with decreases this factor, load carrying capacity in the column decreases, such that reduced by 5.3 % in pure bending moment of column RJRE5 relative to column RJRE2. Ultimate tensile strain of ECC than longitudinal reinforcement and compressive stress of ECC had the least effect on P-M interaction curves.

4.3. Compressive and Tensile Damage of Strengthened Columns

Figures 16 and 17 show compressive and tensile damage of two RJRC and RJRE2 strengthened columns for eccentric load with eccentricity 175 mm. Quantity of compressive and tensile damages for column RJRC is greater than of column RJRE2. Due to the same geometrical properties, and nearly similar behavior of the concrete and ECC materials in stress-strain curve under pressure, difference between the compressive damages is close for the two columns (Fig. 16(a) and Fig. 16(b)), but tensile damages in the columns more varies resulting from difference in tensile behavior for the jacket material (Fig. 17(a) and Fig. 17(b)). Tensile cracks vary in terms of both quantity and distribution of crack. In ECC jacket, tensile cracks were continuous, but in concrete jacket, there were discrete cracks and more of damages.

Table 4. Peak load of columns under concentric or eccentric load (all unites for force is kN).

e(mm)	P_R	P_{RJRC}	P_{RJRE1}	P_{RJRE2}	P_{RJRE3}	P_{RJRE4}	P_{RJRE5}
0	1342.5	3016.7	2883.1	3019.3	3449.2	2756.2	3019.8
40	733.3	2207.3	2100.7	2208	2537.6	1953	2207.5
80	436.5	1554.81	1493.8	1571.6	1890.7	1434.5	1571.5
100	355	1300.81	1280.5	1359.6	1584.2	1229.6	1359.5
120	285.7	1063.5	1073	1163.7	1378.4	1040.6	1163.5
140	228.9	894.89	916	1000.9	1200.6	902.3	1000.7
175	177	673.1	698.3	771.4	992.8	702.8	770.8
220	132.3	495.77	500.5	583	783.6	532.5	560.5

Table 5. Peak moment of columns under eccentric load or pure bending moment (all unites for moment is kN.m).

e(mm)	M_R	M_{RJRC}	M_{RJRE1}	M_{RJRE2}	M_{RJRE3}	M_{RJRE4}	M_{RJRE5}
40	29.3	88.3	84	88.3	101.5	78.1	88.3
80	34.9	124.4	119.5	125.7	151.3	114.8	125.7
100	35.5	130	128	136	158.4	123	136
120	34.3	127.6	128.8	139.6	165.4	124.9	139.6
140	32	125.3	128.2	140.1	168.1	126.3	140.1
175	30.9	117.8	122.2	135	173.7	123	134.9
220	29.1	109	110.1	128.3	172.4	117.2	123.2
∞	23	67.5	67.8	82.8	130.6	78.3	78.4

Table 6. Comparison between reference column and strengthened columns.

e(mm)	P(RJRC/R) or M(RJRC/R)	P(RJRE1/R) or M(RJRE1/R)	P(RJRE2/R) or M(RJRE2/R)	P(RJRE3/R) or M(RJRE3/R)	P(RJRE4/R) or M(RJRE4/R)	P(RJRE5/R) or M(RJRE5/R)
0	2.25	2.15	2.25	2.57	2.05	2.25
40	3.01	2.86	3.01	3.46	2.67	3.01
80	3.56	3.42	3.6	4.33	3.29	3.6
100	3.66	3.66	3.83	4.46	3.46	3.83
120	3.72	3.76	4.07	4.82	3.64	4.07
140	3.9	4	4.38	5.25	3.94	4.38
175	3.81	3.95	4.37	5.62	3.98	4.36
220	3.75	3.78	4.41	5.92	4.03	4.24
∞	2.93	2.95	3.6	5.68	3.4	3.41

5. Theoretical Equations of Concentric Load and Pure Bending Moment for Circular Columns

Theoretical equations are according ACI318-14 [29] and equations Hemmati et al. [37]. Value of concentric load was calculated for reference column and strengthened columns by Eq. (10) and Eq. (11), respectively.

$$P_0 = \alpha_c f_c^{'}.(\frac{\pi D_i^2}{4} - A_{si}) + f_y.A_{si} \quad (10)$$

$$P_0 = \alpha_c f_{cc}^{'}.(\frac{\pi D_i^2}{4} - A_{si}) + \alpha_j f_{cj}.[\frac{\pi}{4}(D_s^2 - D_i^2) - A_{sj}] + f_y.(A_{si} + A_{sj}) \quad (11)$$

In Eq. (10) and Eq. (11), P_0 is concentric load of circular column, D_i is diameter of reference column, A_{si} is total area of longitudinal reinforcement in reference column, D_s is diameter of strengthened column, f_{cj} is peak of compressive stress for jacket material, A_{sj} is total area of longitudinal reinforcement in jacket of strengthened column, coefficient of reduction of compressive stress (α) is obtained by converting stress state from curvature to linear. This coefficient for ECC is a function of peak compressive strain and ultimate compressive strain in ECC [37]. Based on ACI318-14 [29], this coefficient for concrete is equal to 0.85 and for ECC; it is calculated from Eq. (12) as introduced in the study by Hemmati et al. [37].

$$\alpha = \frac{[2/3\varepsilon_{cp} + 0.925.(\varepsilon_{cu} - \varepsilon_{cp})]^2}{2[2/3\varepsilon_{cp}\varepsilon_{cu} + 0.925.(\varepsilon_{cu} - \varepsilon_{cp}) - 5/12\varepsilon_{cp}^{\ 2} - (\varepsilon_{cu} - \varepsilon_{cp})(0.925\varepsilon_{cp} + 2.7/6(\varepsilon_{cu} - \varepsilon_{cp})]} \quad (12)$$

α_c Is coefficient reduction of compressive stress for concrete of reference column and α_j is coefficient reduction of compressive stress for jacket material of strengthened column. When strengthened column is under pure bending moment (M_0), distribution of forces on section column is calculated by Eq. (13) according to Fig. 18 and Fig. 19.

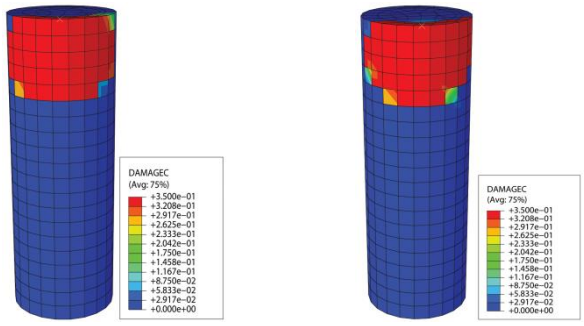

(a) (b)

Fig. 16. Crack pattern and damage quantification at compact for (e=175mm): (a) RJRC column; (b) RJRE2 column.

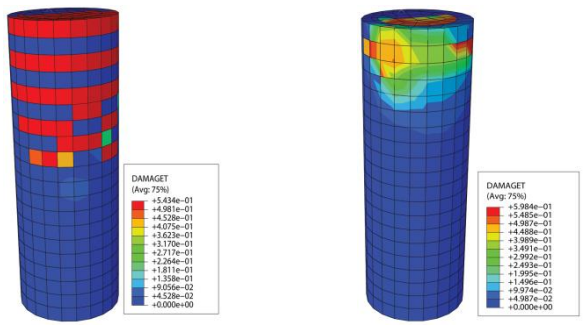

(a) (b)

Fig. 17. Crack pattern and damage quantification at tension for (e=175mm): (a) RJRC column; (b) RJRE2 column.

DOI:10.4186/ej.2020.24.5.77

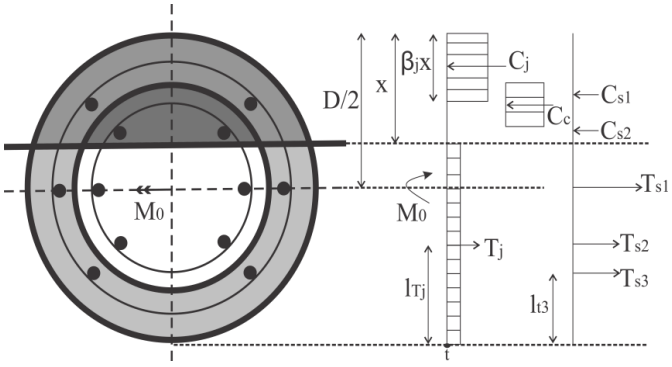

Fig. 18. Distribution of forces on strengthened column under pure bending moment.

As can be seen in Fig.18, concrete has no resistance to tension, but ECC has a resistance to T_j. Value of M_0 obtained from simultaneous solution of two equations. $\sum F_y = 0$, is sum of forces around of y-axis equal to zero, Eq. (14), and $\sum M_t = 0$ is sum moment around of point t equal to zero, calculated by Eq. (15).

In Eq. (15), l is distance of each force to point t. Value of stress in steel reinforcement (under pressure or tension) after calculating strain in steel reinforcement will be calculated according Eq. (16).

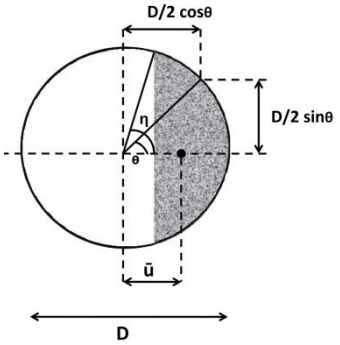

Fig. 19. Characteristics of geometric sector of a circle.

To calculate strain, one should consider linearity of strain variations in height section. In Fig. 18, x is length of the pressure zone. In this regard, to convert curvature of the stress to the line, length of x must be reduced to length of βx (Whitney block) [38]. Value of β for concrete and ECC is calculated by Eq. (17) and Eq. (18), respectively [37].

For calculating pure bending moment of cross section, length of pressure zone of the jacket is column $\beta_j x$ and for reference column is $\beta_c(x - t_j)$. β_j Is coefficient β for jacket of strengthened column, β_c is coefficient β for concrete of reference column and t_j is thickness of jacket

Geometric properties of circular sector are calculated by Eq. (19) and Eq. (20) according to Fig. 19. Table 7 shows exact amount of concentric load (P_0) and Table 8 shows exact amount of pure bending moment (M_0) for reference column and strengthened columns obtained by theoretical and finite element methods. Results obtained from these two methods were also compared.

$$C_c = \alpha_c . f_{cc}^{'} . A_{cc} \ , \quad C_j = \alpha_j . f_{cj} . A_{cj} \tag{13}$$
$$T_j = f_{t0} . A_{tj} \quad , \quad C_s = \sum A_{sc} . f_s$$
$$T_s = \sum A_{st} . f_s$$

In Eq. (13), A_{cc} is area of reference column in compressive zone in length $\beta_c(x - t_j)$ under pure bending moment, A_{cj} is area of jacketing in compressive zone in length $\beta_j x$ under pure bending moment, A_{tj} is area of jacketing in tensile zone under pure bending moment, A_{sc} is area of a longitudinal reinforcement in compressive zone of column under pure bending moment, A_{st} is area of a longitudinal reinforcement in tensile zone of column under pure bending moment, C_c is compressive force of reference column under pure bending moment, C_j is compressive force of jacket column under pure bending moment, T_j is tensile force of jacket column under pure bending moment, C_s is compressive force of a longitudinal reinforcement under pure bending moment, T_s is tensile force of a longitudinal reinforcement under pure bending moment.

$$\sum F_y = 0 \Rightarrow C_c + C_j + C_s - T_j - T_s = 0 \tag{14}$$

$$\sum M_t = 0 \Rightarrow M_0 = C_c . l_{cc} + C_j . l_{cj} + \sum A_{sc} . f_s . l_{sc} - T_j . l_{Tj} - \sum A_{st} . f_s . l_{st} \tag{15}$$

Stress in a steel reinforcement (f_s) (under pressure or tension):

$$f_s = \frac{\varepsilon_s}{\varepsilon_y} . f_y \xleftrightarrow{if} \varepsilon_s < \varepsilon_y \quad , \quad f_s = f_y \xleftrightarrow{if} \varepsilon_s \geq \varepsilon_y \tag{16}$$

Value of β for concrete :(f_c' is expressed in MPa)

$$\beta = 0.85 \xleftrightarrow{if} f_c^{'} \leq 28MPa \tag{17}$$
$$\beta = 0.85 - 0.05.(\frac{f_c^{'} - 28}{7}) \xleftrightarrow{if} 28MPa \leq f_c^{'} \leq 56MPa$$
$$\beta = 0.65 \xleftrightarrow{if} f_c^{'} \geq 56MPa$$

Value of β for ECC:

$$\beta = \frac{2[2/3\varepsilon_{cp}\varepsilon_{cu} + 0.925.(\varepsilon_{cu} - \varepsilon_{cp}) - 5/12\varepsilon_{cp}^{\ 2} - (\varepsilon_{cu} - \varepsilon_{cp})(0.925\varepsilon_{cp} + 2.7/6(\varepsilon_{cu} - \varepsilon_{cp})]}{\varepsilon_{cu}[2/3\varepsilon_{cp} + 0.925.(\varepsilon_{cu} - \varepsilon_{cp})]} \tag{18}$$

Geometric properties sector of circle:

$$A_c = \frac{D^2}{2}\int_0^{\eta} \sin^2\theta.d\theta = D^2\left[\frac{\eta - \sin\eta.\cos\eta}{4}\right] \quad (19)$$

$$A_c.\bar{u} = \frac{D^3}{4}\int_0^{\eta} \sin^2\theta.\cos\theta.d\theta = D^3\left[\frac{\sin^3\eta}{12}\right] \quad (20)$$

In Eq. (19) and Eq. (20), A_c is area of sector of circular, $\bar{u}$ is from centre to centre of circular and sector of circular (Fig. 19).

According Table 7, difference between results obtained from finite element and theoretical methods is between 2-8% for columns under concentric load. Difference between results can be logical and acceptable. This difference according Table 8 between results for columns under pure bending moment was between 10-14%. This difference may be due to post yielding increase in tensile reinforcement, converting stress surfaces from curvature to line with coefficients of α and β (Whitney block), complete ignoring of concrete under tension and considering a constant value for tensile stress of ECC (f_{t0}), while varying between f_{t0} and f_{tu}.

With all simplifications made in theory equations for columns under pure bending moment, this amount of difference can be logical and reliable regarding accuracy of results obtained from finite element and theoretical methods for reference column and strengthened columns.

Table 7. Comparison Theo. and FE results for circular columns under concentric load (all unites are kN for P_0).

Columns	P_0(Theo.)	P_0(FE)	P_0(Theo./FE)
R	1228.5	1342.5	0.92
RJRC	2868.4	3016.7	0.95
RJRE1	2840.2	2883.1	0.98
RJRE2	2948.6	3019.3	0.97
RJRE3	3296	3449.2	0.95
RJRE4	2523.4	2756.2	0.92
RJRE5	2948.6	3019.8	0.97

Table 8. Comparison Theo. and FE results for circular columns under pure bending moment (all unites are kN.m for M_0).

Columns	M_0 (Theo.)	M_0 (FE)	M_0 (Theo./FE)
R	20.5	23	0.89
RJRC	58.6	67.5	0.87
RJRE1	59.8	67.8	0.88
RJRE2	73.3	82.8	0.89
RJRE3	112.4	130.6	0.86
RJRE4	68.1	78.3	0.87
RJRE5	71.2	78.4	0.9

6. Conclusions

The use of ECC for strengthened of reinforced concrete columns is interesting, due to its similar structure and strong connection to concrete. The following conclusions can be drawn according to study on strengthening of reinforced concrete columns:

1- Strengthened methods used in this study increased load carrying capacity of the reference column from 2 to 5.92 times. Exact value of this increase depends on type of strengthening and eccentricity of eccentric load. Also, by increasing eccentricity of eccentric load due to bending moment in addition to axial load, loading capacity decreased in the column. Value of this reduction for the R column at eccentric load with eccentricity 220 mm is one tenth of the concentric load.

2- In columns strengthened with concrete or ECC jacketing, due to almost similar compressive behavior of concrete and ECC and geometrical properties of the columns, the concentric load-axial displacement curves of the two columns coincide. Difference in the column loading capacity begins when there is considerable tension in the column. By increasing eccentricity from eccentric load, load carrying capacity in column strengthened with ECC jacketing increased from 0.4-23% times similar to the strengthened of column with concrete jacketing, attributing to occurrence of tensile strain hardening behavior of this material after formation of the first tensile crack in ECC. Difference between of compressive damages is close in jacketing concrete and ECC, but in tensile damages more vary in terms of both quantity and distribution of crack. In ECC jacketing, tensile cracks are continuous but in concrete jacketing, there are discrete cracks and more damages.

3- Effect of increasing compressive stress of ECC in jacketing layer was greater in pressure region than tensile region in P-M interaction curve. By increasing compressive strength of ECC jacketing from 25 to 35 MPa, eccentric load at eccentricity of 40 mm and pure bending moment increased to 13 and 5.6%, respectively.

4- With an approximately 2.8-time increase in the area of longitudinal reinforcement at ECC jacketing, load carrying capacity increased, that it is value varies. In concentric load, it creased to 13%, and in pure bending moment, it increased to 58%. Effect of increasing longitudinal reinforcement in ECC jacketing in tension control region was greater than pressure control region in P-M interaction curve.

5- Ultimate tensile strain of ECC was effective on load carrying capacity of strengthened column. Importance of this variable is obvious in eccentric compression load with high eccentricity. Also, compared to other variables studied, this variable had the least effect on P-M interaction curve.

References

[1] A. Sichko and H. Sezen, "Review of methods for reinforced concrete column retrofit," in *SMAR 2017- Fourth Conference on Smart Monitoring, Assessment and Rehabilitation of Civil Structures*, Zurich, Switzerland, 2017.

[2] E. S. Júlio, F. Brancoand, and V. D. Silva, "Structural rehabilitation of columns with reinforced concrete jacketing," *Progress in Structural Engineering Materials Banner – Repair and Rehabilitation*, vol. 5, pp. 29–37, 2003.

[3] R. Dubey and P. Kumar, "Experimental study of the effectiveness of retrofitting RC cylindrical columns using self-compacting concrete jackets," *Construction and Building Materials*, vol. 124, pp. 104-117, Oct. 2016.

[4] M. Haji, H. Naderpour, and A. Kheyroddin, "Experimental study on influence of proposed FRP-strengthening techniques on RC circular short columns considering different types of damage index," *Composite Structure*, vol. 209, pp. 112-128, Feb. 2019.

[5] M. N. S. Hadi, T. M. Pgam, and X. Lei, "New method of strengthening reinforced concrete square columns by circularizing and wrapping with fibre reinforced polymer or steel straps," *Journal of Composite for Construction*, vol. 17, no. 2, pp. 229-238, Apr. 2013.

[6] S. Panyamul, P. Panyakapo, and A. Ruangrassamee, "Seismic shear strengthening of reinforced concrete short columns using ferrocement with expanded metal," *Engineering Journal*, vol. 23, no. 6, pp. 176-189, Nov. 2019.

[7] M. F. Belal, H. M. Mohamed, and S. A. Morad, "Behavior of reinforced concrete columns strengthened by steel jacket," *HBRC Journal*, vol. 11, no. 2, pp. 201-212, Aug. 2015.

[8] G.T. Truong, J.C. Kim, K.K. Choi, "Seismic performance of reinforced concrete columns retrofitted by various methods", *Engineering Structure*s, vol. 134, pp. 217-235, Mar., 2017.

[9] *Repair and Strengthening of Reinforced Concrete Columns and Beams*, International Concrete Repair Institute Transportation Structures, ICRI, 2010.

[10] H. Hu, M. ASCE, C. S. Huang, M. H. Wu, and Y. M. Wu, "Nonlinear analysis of axially loaded concrete-filled tube columns with confinement effect," *Structure Engineering*, vol. 129, no. 10, pp. 1322-1329, Oct. 2003.

[11] B. Gencturk and A. S. Elnashai "Numerical modelling and analysis of ECC structures," *Materials and Structures*, vol. 46, no. 4, pp. 663-682, Apr. 2013.

[12] G. Fischer and V. C. Li, "Structural composites with ECC," in *Proceedings of the ASCCS-6*, 2000, pp. 1001-1008.

[13] E. Parsa, M. K. Sharbtdar, and A. Kheyroddin, "Investigation of flexural behavior of RC frames strengthened with HPFRCC subjected to lateral loads," *Iranian Journal of Science and Technology, Transactions of Civil Engineering*, vol. 43, no. 2, pp. 231-240, Jun. 2019.

[14] F. Yuan, M. Chen, F. Zhou, and C. Yang, "Behaviors of steel-reinforced ECC columns under eccentric compression." *Construction and Building Materials*, vol. 185, pp. 402-413, Oct. 2018.

[15] K. M. Quang, V. B. P. Dang, S. W. Han, M. Shin, and K. Lee, "Behavior of high-performance fiber-reinforced cement composite columns subjected to horizontal biaxial and axial loads," *Construction and Building Materials*, vol. 106, pp. 89-101, Mar. 2016.

[16] P. Jinlong, G. Jie, and C. Junhun, "Theoretical modeling of steel reinforced ECC column under compressive loading," *Science China Technological Sciences*, vol. 58, pp. 889-898, May 2015.

[17] A. Hemmati, A. Kheyroddin, M. Sharbatdar, Y. Purk, and A. Abolmali, "Ductile behavior of high performance fiber reinforced cementitious composite (HPFRCC) frames," *Construction and Building Materials*, vol. 115, pp. 681-689, Jul. 2016.

[18] P. Ramadoss and K. Nagamani, "Tensile strength and durability characteristics of high-performance fibre reinforced concrete," *Arabian Journal for Science and Engineering*, vol. 33, no. 2B, pp. 307–319, Jan. 2008.

[19] W. Wanga, J. Liub, F. Agostini, C. A. Davy, F. Skoczylas, and D. Corvez, "Durability of an ultra-high performance fibre reinforced concrete (UHPFRC) under progressive aging," *Cement and Concrete Research*, vol. 55, pp. 1–13, Jan. 2014.

[20] C. Shim, C. Koem, H. H. Song, and S. Park, "Seismic severely damaged precast columns with high-fiber reinforced cementitious composites," *KSCE Journal of Civil Engineering*, vol. 22, no. 2, pp. 736-746, Feb. 2018.

[21] A. Meda, S. Mostosi, Z. Rinaldi, and P. Riva, "Corroded RC columns repair and strengthening with high performance fiber reinforced concrete jacket," *Materials and Structures*, vol. 49, no. 5, pp. 1967-1978, May 2016.

[22] *ABAQUS (6.12. SimuliaInc).* Providence, RI, 2012.

[23] *Help of ABAQUS, Getting Started with ABAQUS*. 2012.

[24] A. Hemmati, A. Kheyroddin, and M. K. Sharbatdar, "Increasing the flexural capacity of RC beams using partially HPFRCC layers," *Computer and Concrete*, vol. 16, pp. 545-568, 2015.

[25] A. Hemmati, A. Kheyroddin, and M. K. Sharbatdar, "Flexural behavior of reinforced HPFRCC beams," *Journal of Rehabilitation in Civil Engineering*, vol. 1, pp. 66-77, Jan. 2013.

[26] A. He, J. Cai, Q.J. Chen, X. Liu, H. Xue, and C. Yu, "Axial compressive behavior of steel-jacket retrofitted RC columns with recycled aggregate concrete," *Construction and Building Materials*, vol. 141, pp. 501-516, Jun. 2017.

[27] M. Elchalakani, A. Karrech, M. Dong, M. S. Mohamed Ali, and B. Yang, "Experiments and finite element analysis of GFRP reinforced geopolymer

concrete rectangular columns subjected to concentric and eccentric axial loading," *Structure Journal*, vol. 14, pp. 273-289, Jun. 2018.

[28] M. Chellapandian, S. SuriyaPrakash, and A. Rajagopal, "Analytical and finite element studies on hybrid FRP strengthened RC column elements under axial and eccentric compression," *Composite Structures*, vol. 184, pp. 234-248, Jan. 2018.

[29] *Building Code Requirements for Structural Concrete and Commentary on Building Code Requirements for Structural Concrete*, American Concrete Institute (ACI), Farmington Hills, MI, ACI318, 2014.

[30] W. Anuntasena, A. Lenwari, and T. Thepchatri, "Finite element modelling of concrete-encased steel columns subjected to eccentric loadings," *Engineering Journal*, vol. 23, no. 6, pp. 300-310, Nov. 2019.

[31] M. A. Shayanfar, A. Kheyroddin, and M. S. Mirza, "Element size effects in nonlinear analysis of reinforced concrete members," *Computers & Structures*, vol. 62, no. 2, pp. 339-352, 1997.

[32] A. Kheyroddin, "Nonlinear finite element analysis of flexure-dominant reinforced concrete structures," Ph.D. thesis, McGill Univ., Montréal, 1996.

[33] C. G. Cho, Y. Y. Kim, L. Feo, and D. Hui, "Cyclic responses of reinforced concrete composite columns strengthened in the plastic hinge region by HPFRC mortar," *Composite Structures*, vol. 94, pp. 2246-2253, Jun. 2012.

[34] P. C. Rodrigues and D. L. Araujo, "Analysis of the efficiency of strengthening design models for reinforced concrete columns," *IBRACON Structures and Materials Journal*, vol. 11, no. 6, pp. 1418-1452, Dec. 2018.

[35] *Federation International du Beton (FIB)*, model code 2010–final draft, vol. 2, pp. 16-26, 2012.

[36] G. Campione, "The effects of fibers on the confinement models for concrete columns," *Canadian Journal of Civil Engineering,* pp. 742-750, Sep. 2002.

[37] A. Hemmati, A. Kheyroddin, and M. K. Sharbatdar, "Proposed equations for estimating the flexural characteristics of reinforced HPFRCC beams," *Iranian Journal of Science and Technology, Transactions of Civil Engineering*, vol. 38, no. C2, pp. 395-407, Aug. 2014.

[38] H. A. Hamid and S.D. Mohammed, "Flexural moment capacity evaluation of reinforced reactive powder concrete two-way slabs," *Engineering Journal*, vol. 23, no. 1, pp. 109-121, Jan. 2019.

Mohammad Javad Memar, photograph and biography not available at the time of publication.

Ali Kheyroddin, photograph and biography not available at the time of publication.

Ali Hemmati, photograph and biography not available at the time of publication.